RSC Advances

PAPER

View Article Online
View Journal | View Issue

Cite this: *RSC Adv.*, 2024, **14**, 36930

Upconverting particles in near-infrared light-induced TiO_2 photocatalysis: towards the optimal architecture of upconverter/photocatalyst systems†

Paulina O'Callaghan,[a] Agnieszka Jarosz-Duda,[a] Joanna Kuncewicz,[a]* Krzysztof Dzierżęga[b] and Wojciech Macyk[a]*

Received 7th June 2024
Accepted 30th October 2024

DOI: 10.1039/d4ra04185b

rsc.li/rsc-advances

Preparation of highly active core–shell/hybrid materials based on up-converting particles combined with semiconductors for photocatalytic application usually requires sophisticated and multi-step synthesis procedures. We propose a new design of a highly efficient NIR-driven photocatalytic system composed of spatially separated thin films of upconverting $NaYF_4$:Yb,Tm particles (UCPs), and TiO_2. Several samples of UCPs were prepared in the form of thin films and suspensions, directly coated with a titania layer or mixed with P25. Photocatalytic and photoelectrochemical studies have shown that thin film samples achieved significantly higher photocatalytic activity than their suspended counterparts. Moreover, the sample consisting of spatially separated layers of UCPs and P25 presented a significant photocatalytic activity and generated the highest photocurrent intensity. Separating the photocatalyst and upconverter layers allows for an interchangeable photocatalytic system active in a wide range of light.

Introduction

Some of the most extensively studied photocatalytic systems based on upconverting particles are composites of $NaYF_4$:Yb,Tm particles and TiO_2.[1–5] The $NaYF_4$:Yb,Tm crystals, absorbing at 980 nm, emit light in the UV/Vis/NIR range which can be utilized to excite the photocatalyst.[6] In such hybrid systems, a photocatalyst is usually loaded on the surface of the UCPs.[7,8] It is believed that such heterostructured architecture provides the required contact between the components. In some cases, it may even enable the energy transfer among components and thus improve the photocatalytic activity of the materials.[9] However, these systems often suffer from low efficiency.[10,11] Many efforts have been made to increase the photocatalytic activity of UCP-based photocatalysts under NIR irradiation.[12,13] These studies are mainly focused on improving the efficiency of the upconverting materials by, *e.g.*, developing new core–shell structures, combining the UCPs with photonic crystals, or enhancing absorption of the light emitted by UCPs by photocatalysts through, for example, their combination with plasmonic nanoparticles or dye photosensitizers.[14–22] Moreover, nano-sized UCPs/photocatalyst materials are desired since excitation of the suspension of micro-sized particles with a high density-NIR light source, which is necessary for multi-photon processes, is impeded due to the intense light scattering.

In our work, we propose a different approach. We demonstrate that high photocatalytic activity of the UCPs-based photocatalysts can be achieved without changing the chemical or spectroscopic properties of their components, *e.g.* by synthesis of the additional shells, modifications, or dopants, which only increase the complexity of the structure. Moreover, we propose a design of a highly efficient NIR-driven photocatalytic system with spatially separated and fully interchangeable components. In the proposed systems no physical contact, *i.e.* heterojunction, between the components is necessary to preserve desired photocatalytic activity.

Results and discussion

Synthesis, morphology, elemental and structural analysis

We synthesized $NaYF_4$:Yb,Tm particles and combined them with a semiconductor by either directly synthesizing the titania shell (UCPs@TiO_2) or by mixing them with commercial TiO_2 (P25, Evonik) (UCPs + P25). The obtained UCPs crystals are in the form of microrods with an average length of approximately 1.5 μm and a diameter of roughly 0.3 μm (Fig. 1a). The surface of pure UCPs appears to be smooth, and the crystals are well-developed. The mixture of the UCPs and P25 is inhomogeneous on a microscale and shows two fractions – tiny TiO_2 crystals and $NaYF_4$:Yb^{3+},Tm^{3+} microrods (Fig. 1b). Deposition of

[a]*Faculty of Chemistry, Jagiellonian University, ul. Gronostajowa 2, 30-387 Kraków, Poland. E-mail: kuncewic@chemia.uj.edu.pl; macyk@chemia.uj.edu.pl*

[b]*Faculty of Physics, Astronomy and Applied Computer Science, Jagiellonian University, ul. Łojasiewicza 11, 30-348 Kraków, Poland*

† Electronic supplementary information (ESI) available. See DOI: https://doi.org/10.1039/d4ra04185b

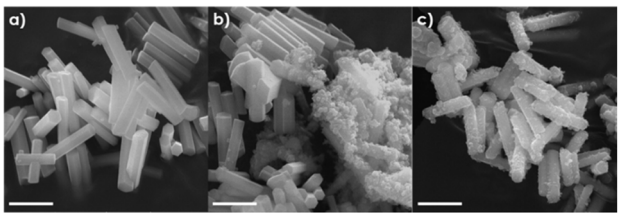

Fig. 1 SEM images of (a) uncoated UCPs, (b) UCPs mixed with P25 and (c) UCPs coated with TiO_2 layer. The scale bar represents 1 μm.

TiO_2 on the pure UCPs crystals by solvothermal method followed by the calcination resulted in the formation of a uniform layer of anatase TiO_2 nanoparticles (sample β-$NaYF_4$:Yb^{3+},Tm^{3+}@TiO_2, Fig. 1c), which was confirmed by the XRD and EDX analysis (Fig. 2 and S1c,† respectively).

The diffractogram of the β-$NaYF_4$:Yb^{3+},Tm^{3+} sample represents very sharp diffraction peaks assigned to hexagonal crystalline structure (β-$NaYF_4$, PDF no. 00-064-0156), indicating the excellent crystallinity of the synthesized material. No impurities from the cubic phase (α-$NaYF_4$:Yb^{3+},Tm^{3+}) crystals were detected. The size and crystalline structure of upconverting microcrystals combined with TiO_2 were neither affected by the solvothermal synthesis of TiO_2 nor the calcination process (Fig. 2).

Spectroscopic analysis

$NaYF_4$ doped with Yb^{3+} and Tm^{3+} ions emits light within UV and visible range under a 980 nm laser excitation, as shown in Fig. 3a. The UV emission peaks with maxima at 349 and 362 nm, which are crucial for the NIR-driven photocatalytic activity of TiO_2, are attributed to the five- and four-photon transitions of Tm^{3+} ions: $^1I_6 \rightarrow {}^3F_4$, and $^1D_2 \rightarrow {}^3H_6$, respectively. The two blue emission peaks centered at 450 and 474 nm correspond to the four- and three-photon $^1D_2 \rightarrow {}^3F_4$ and $^1G_4 \rightarrow {}^3H_6$ transitions of Tm^{3+} ions, respectively. The measurements of luminescence were performed for the materials in the form of thin films (f; *cf.* caption to Fig. 3) spread on ITO foil. Some significant spectral differences can be observed between the UCPs samples coated or mixed with titania and pure UCPs. The intensities of the emission bands in the UV range decrease for both UCPs@TiO_2(f) and UCPs + P25(f), while the emission intensity of the band centered at 476 nm remains almost unaffected compared with the pure UCPs. The observed attenuation of the UV emission has arisen from the absorption of the light emitted by upconverting crystals by the TiO_2, which was indicated by the DRS spectra of the UCPs samples (Fig. 3b). However, the reduction of the UV emission is more pronounced in the case of UCPs + P25(f) than for UCPs@TiO_2(f), which may result from a weaker absorption of the UV light by the deposited TiO_2. Moreover, the intensity of the 452 nm emission band with respect to the 476 nm band, which indicates the efficiency of four-photon transition, is significantly lower for UCPs@TiO_2(f) than for UCPs + P25(f).

The efficiency of multi-photon processes strongly depends on the host's crystal field and geometry, concentration and spatial arrangement of the luminescent ions, particularly the

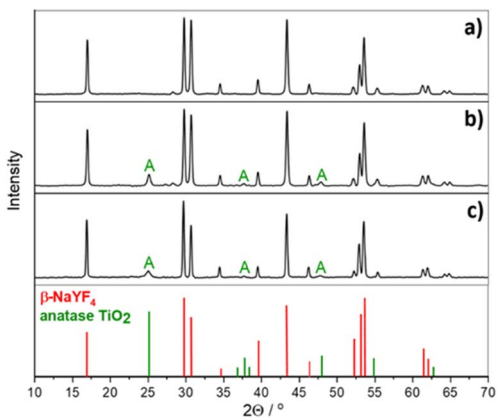

Fig. 2 XRD patterns of (a) UCPs (β-NaYF4:Yb^{3+},Tm^{3+}) crystals, (b) UCPs + P25 (β-$NaYF_4$:Yb^{3+},Tm^{3+} mixed with P25) sample and (c) UCPs@TiO_2 (β-$NaYF_4$:Yb^{3+},Tm^{3+} coated with TiO_2) sample. "A" indicates reflections characteristic for TiO_2 anatase.

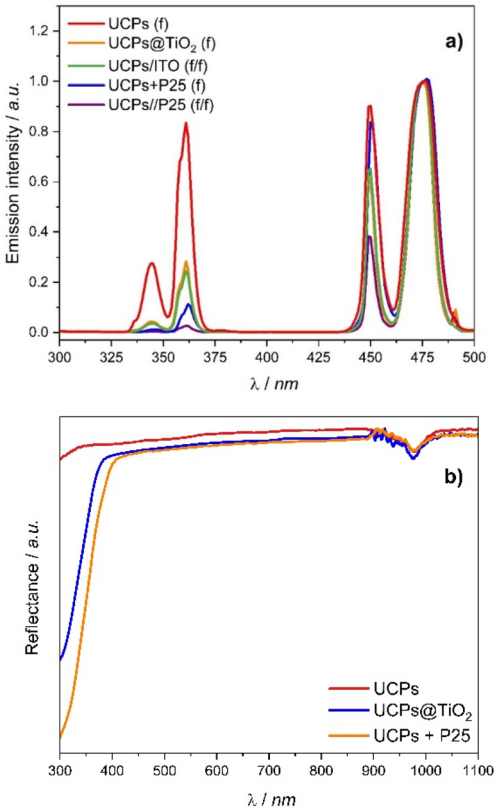

Fig. 3 (a) Upconversion luminescence spectra of UCPs crystals (UCPs(f)), UCPs coated with titania (UCPs@TiO_2(f)), UCPs mixed with P25 (UCPs + P25(f)), spatially separated UCPs and P25, deposited on two different ITO foil pieces (UCPs/P25(f/f)) and UCPs with additional uncoated ITO substrate (UCPs/ITO(f/f)). All spectra have been normalized to the emission intensity at 476 nm. (b) The DRS spectra of the UCPs, UCPs coated with titania layer (UCPs@TiO_2), and UCPs mixed with P25 (UCPs + P25). The 980 nm band originates from the Yb^{3+} absorption. Tauc plots of UCPs@TiO_2 and UCPs + P25 are presented in Fig. S2.†

presence of the volume and surface defects.[23] The lower efficiency of upconversion arising from the four-photon transition observed for UCPs@TiO_2 may result from the structural changes in UCPs particles caused by the TiO_2 deposition process, which did not occur in the case of the UCPs + P25 physical mixture. A significant decrease in the UV emission intensity was also observed for the sample where UCPs and P25 films are spatially separated (UCPs/P25(f/f); *cf.* ESI†). Apart from the strong absorption of the UV light by P25, an additional reduction of visible light emission intensity was observed. In UCPs/P25(f/f) sample, incident light passes through the ITO foil covered with P25 before reaching the UCPs film. The attenuation of the visible light emission indicates partial absorption of the incident NIR light by ITO foil. It was confirmed by the decrease of intensities of all (349, 362, and 452 nm) peaks observed in the spectrum of UCPs thin film with the uncoated ITO foil placed in front of the sample (UCPs/ITO(f/f)).

Photoelectrochemical measurements

The same samples in the form of films were used in photoelectrochemical measurements to quantify the generation of electron–hole pairs in the UCPs-based photocatalytic systems under NIR light (Fig. 4). We observed repetitive photocurrent pulses from electrodes in response to laser pulses. The samples containing P25 (UCPs + P25(f) and UCPs/P25(f/f)) exhibit much stronger photocurrents than in the case of the UCPs@TiO_2 sample, which indicates the advantage of mixed systems over coated ones. Although identical amounts of the UCPs and TiO_2 were used for the preparation of UCPs + P25(f) and UCPs/P25(f/f) samples, the highest photocurrents were achieved for the sample where P25 was spatially separated from the UCPs layer. It is most likely because the electron transport through the electrode was not obstructed by the UCPs crystals dispersed in the semiconductor layer. Due to the spatial separation, the TiO_2 layer was uniformly irradiated, and more semiconductor particles were in direct contact with the underlying ITO layer and electrolyte. The bare P25 and UCPs samples show scarcely any photo-response under NIR irradiation.

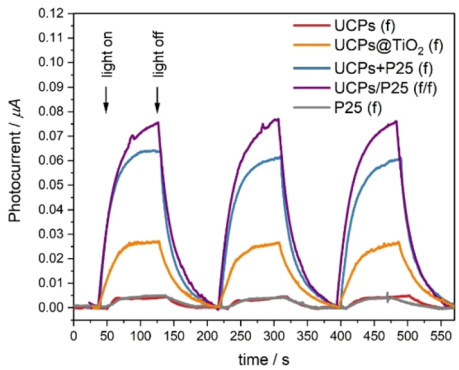

Fig. 4 Photocurrent response of UCPs, UCPs coated with titania (UCPs@TiO_2(f)), UCPs mixed with P25 (UCPs + P25(f)), spatially separated UCPs and P25 deposited on two different ITO foil pieces (UCPs/P25(f/f)) and P25 under 980 nm excitation.

Photocatalytic performance

It has been reported that $NaYF_4$:Yb^{3+},Tm^{3+} crystals directly coated with titania act as a more efficient photocatalyst compared with their physical mixture with TiO_2.[24–26] However, most of the papers on the titania-coated upconversion-based photocatalysts present the results of the photocatalytic test of colloidal solutions/suspensions of those materials.[25,27,28] In our work, the photoactivity of the $NaYF_4$:Yb^{3+},Tm^{3+} combined with TiO_2 in the forms of suspended powders (s) and thin films (f) has been studied in various arrangements (Fig. 5). To verify the photocatalytic activity of examined samples, terephthalic acid (TA) was used as a probe compound to estimate of $HO^{\bullet}$ radicals generation efficiency. TA reacts with photogenerated radicals to form a luminescent hydroxyterephthalic acid (TAOH).

Fig. 6 shows the time dependence of the concentration of the generated TAOH upon NIR irradiation. Firstly, the results demonstrate that the materials in the form of thin films exhibit remarkably higher photocatalytic activity under NIR irradiation than their suspended counterparts. Irradiation of the UCPs@TiO_2(s) (setup 1) generated an insignificant amount of hydroxyl radicals. However, the measured photocatalytic activity increased significantly when the same amount of the material was irradiated as a thin film (setup 2). It is most likely due to the substantial reduction of the solvent-based radiation losses in

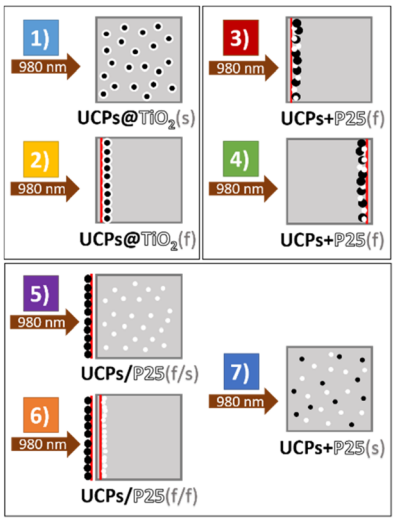

Fig. 5 A graphical representation of the used experimental setups of the photocatalytic activity measurements. A brown arrow represents a light beam of a 980 nm laser diode, aiming towards the glass cuvette, depicted as a square. A red line represents PE foil covered with ITO substrate. The cuvettes were filled with 0.3 mM TA solution and the materials were either suspended in it (setups 1, 5, 7) or immersed as thin films on an ITO foil (depicted as setups 2, 3, 4, 6). The black and white colors correspond to UCPs and titania, respectively. The position of the vertical lines covered with particles of the material represents the position of the sample on the ITO foil *versus* the cuvette. (1) UCPs@TiO_2(s) suspension, (2) UCPs@TiO_2(f) thin film, (3) UCPs + P25(f) thin film positioned closer to the front cuvette wall, (4) UCPs + P25(f) thin film positioned closer to the back cuvette wall, (5) UCPs thin film in front of the cuvette and P25 suspension inside (UCPs/P25(f/s)), (6) UCPs thin film in front of the cuvette and P25 thin film inside (UCPs/P25(f/f)), (7) suspension of the UCPs and P25 physical mixture (UCPs + P25(s)).

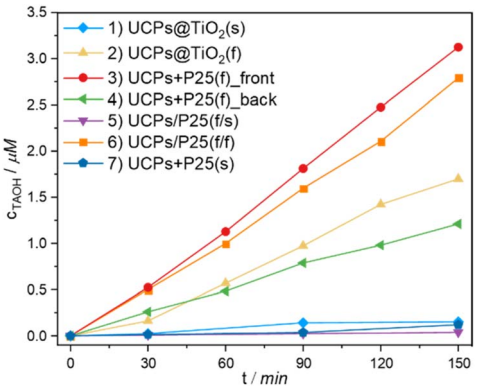

Fig. 6 The concentration of TAOH generated in the presence of studied materials in the experimental setups depicted in Fig. 5 (1–7), under 980 nm irradiation.

the thin film system. The intensity of the upconversion (I_{UC}) emission strongly depends on the intensity of the excitation light (I), according to eqn (1):[1]

$$I_{UC} = k \cdot I^n \quad (1)$$

where k is a material-related constant and n is the number of photons involved in the upconversion process. This dependency is particularly significant in the case of the processes arising from four- or even five-photon absorption, like the UV emission. Water is a solvent that strongly absorbs radiation at 980 nm.[29] The measured 980 nm light intensity at the output of the cuvette with aqueous TA solution was almost two times lower than at the input. The detrimental effect of the water absorption of the incident light is demonstrated in the results of the photocatalytic tests of the sample UCPs + P25(f) in setups no. 3 and 4. Placing the sample at the back of the cuvette (setup no. 4) resulted in a considerable decrease in its photocatalytic activity. Another reason for the scarce photocatalytic activity of the materials in the suspensions or colloidal solutions is a considerably lower concentration of the particles in the area irradiated with the emitted UV or incident NIR light compared to thin films. Moreover, every non-radiative de-excitation resulting from, *e.g.*, quenching at the solvent molecules may lower the intensity of the up-converted light.[30,31] The advantage of thin films is also the possibility of using a much smaller amount of material compared to suspensions and reusing both materials after the experiment. The used material also does not have to be nanometric. Our results also show that it is not necessary, and sometimes even disadvantageous, to deposit the photocatalyst directly on the surface of the upconverting particles. The UCPs@TiO_2(f) sample (setup no. 2) exhibited lower photocatalytic activity than the UCPs mixed with P25 (UCPs + P25(f), setup no. 3), which is in agreement with the photoelectrochemical measurements. Apart from the lower absorption of emitted UV light by the TiO_2 shell compared with the P25 component, the surface coating with a photocatalyst layer is yet another step of the synthesis, which makes the process longer and more expensive. Moreover, each step can lead to the introduction of bulk and surface defects to the structure of UCPs and modify their spectroscopic properties. Moreover, the as-synthesized photocatalyst is most likely to be of inferior quality compared to P25, which is one of the most efficient commercially available photocatalysts.[32]

The obtained results not only demonstrate the superiority of the films of physical mixtures of UCPs/photocatalyst over the films of hybrid materials obtained in a multi-step process but also unequivocally show no need for direct contact between the UCPs and the photocatalyst. The high photocatalytic activity of setup 6, when the photocatalyst and UCPs layers are separated physically by a quartz wall of the cuvette, proves that the mechanism of TiO_2 excitation involves the emission of UV light by UCPs and its absorption by titania particles (both confirmed by spectroscopic measurements). No other energy or electron transfer processes can occur through a thick (*ca.* 1.25 mm) quartz window. This shows that in the case of such hybrid semiconductor/UCPs materials, the heterojunction created between the components is irrelevant to overall activity because no electron transfer between them is necessary. In addition, in such systems with spatially separated components, it is possible to use various photocatalysts with the same film of UCPs and change them when necessary. Such design allows for the creation of interchangeable and reusable NIR-driven photocatalytic systems.

Experimental

Materials

Ytterbium chloride hexahydrate ($YbCl_3 \cdot 6H_2O$, 99.99%, Sigma-Aldrich), yttrium chloride hexahydrate ($YCl_3 \cdot 6H_2O$, 99.99%, Sigma-Aldrich), thulium chloride anhydrous ($TmCl_3$, 99.99%, Sigma-Aldrich), sodium hydroxide (NaOH, 99.8%, POCh), oleic acid (OA, 99.9%, Fluka), ammonium fluoride (NH_4F, Acros), ethyl alcohol (EtOH, POCh), cyclohexane (Sigma-Aldrich), hydrochloric acid (HCl, POCh), terephthalic acid (TA, Aldrich), and titanium(IV) oxide (P25, Evonik), titanium(IV) fluoride (TiF_4, Sigma-Aldrich), polyvinylpyrrolidone (PVP10, Sigma-Aldrich), barium sulfate ($BaSO_4$, Sigma-Aldrich) were used as received without further purification.

Synthesis of $NaYF_4$:Yb^{3+},Tm^{3+} microcrystals (UCPs)

The $NaYF_4$:Yb,Tm phosphors were prepared by a solvothermal method. In a typical process, 0.36 g NaOH was transferred to a Teflon autoclave lining, filled with 2.4 ml ethanol and 0.6 ml distilled water, and stirred until a homogeneous solution was obtained. Vigorous stirring was continued throughout the preparation of the reaction mixture. Then 6 ml of oleic acid was added to the solution. After 20 minutes, a total volume of 1.5 ml of 0.2 M rare-earth chlorides solutions (YCl_3, $YbCl_3$, and $TmCl_3$ with a stoichiometric ratio of 50 : 49 : 1) was added dropwise to the reaction vessel. The amount of the added 0.1 M NH_4F was fixed at 2.4 ml for obtaining particles with $F^-/RE^{3+} = 8/1$ molar ratio.

The Teflon lining with the resulting solution was then placed in a stainless steel autoclave, sealed, and maintained at 190 °C

for 12 hours. The synthesized particles were washed with ethanol and centrifuged at 5000 rpm for 20 minutes. The supernatant was removed, and the particles were washed several times with cyclohexane and ethanol to remove the remaining unbound oleic acid and possible impurities formed during the synthesis. The purified oleate-capped particles were collected and dried in the oven at 60 °C. To remove oleic acid from the surface of $NaYF_4$:Yb^{3+},Tm^{3+} crystals to obtain ligand-free water-dispersible upconverting microcrystals, the modified literature procedure reported by Bogdan *et al.* was used.[33] In a typical experiment, oleate-capped particles were dispersed in 2 ml of 2 M HCl solution and sonicated for 15 min to remove surface ligands. The products were washed with ethanol and water three times, collected by centrifugation, and dried in the oven at 60 °C. To improve the crystallinity of the materials and remove any organic impurities, the obtained powders were calcined in the oven at 400 °C for 3 hours.

Synthesis of $NaYF_4$:Yb^{3+},Tm^{3+}@TiO_2 composites (UCPs@TiO_2)

The $NaYF_4$:Yb^{3+},Tm^{3+}@TiO_2 composites were synthesized according to a modified literature procedure.[34] In a typical experiment, 25 mg of the previously synthesized upconverting particles were mixed with 3 ml of deionized water and 0.3 g of PVP. The mixture was sonicated until all of the PVP was dissolved. Subsequently, 10 ml of ethanol was added to a reaction flask, and the content was stirred for 30 minutes. As a titanium source, 4 ml 0.025 M TiF_4 solution was added dropwise. The reaction content was transferred into a 20 ml Teflon-lined steel autoclave and maintained at 180 °C for 6 h. After cooling to room temperature, the obtained products were precipitated with ethanol, centrifuged at 3300*g* for 10 minutes, and washed with DI water and ethanol three times. The particles were then dried on air and further calcined in the oven at 400 °C for 3 hours.

Preparation of the thin films of the materials

The mixture of the UCPs and P25 (UCP + P25) was prepared by grinding in a mortar 2 mg of the UCPs with 1 mg of P25. Then, 20 μl of water was added, and the suspension was transferred on the ITO foil and spread evenly to form a uniform layer of the area matching the beam size (*vide infra*). The film was then dried in a stream of warm air (*ca.* 40–50 °C). To prepare a sample composed of spatially separated UCPs and TiO_2 (P25), labelled UCPs/P25, 2 mg of UCPs and 1 mg of P25 were ground and loaded onto separate ITO foil sheets and then dried. The thin film of UCPs coated with titania (UCPs@TiO_2) was prepared correspondingly, with 3 mg of the material loaded onto the ITO foil.

Characterization

The purity and phase structure of the synthesized particles were obtained using a MiniFlex 600 (Rigaku) X-ray diffractometer equipped with CuK_α nickel-filtered source lamp (λ = 1.54 Å) operating at 40 kV voltage. The scan range was 3–70° 2θ with a step of 0.02° and a speed of 10° per minute.

The size, morphology, and elemental analyses were determined using a Vega 3 LM (Tescan) scanning electron microscope equipped with a LaB_6 cathode and EDS detector (10 mm^2 x-act SDD detector, Oxford Instruments) operating at 20 and 30 kV voltage. The samples were prepared by spreading the powders on carbon tape.

PerkinElmer LS55 fluorescence spectrometer was used to record luminescence spectra of hydroxyterephthalic acid. The excitation wavelength was set to 315 nm, and emission was measured in the 300–600 nm range. The measurements were performed in high-purity cuvettes with a path length of 1 cm.

The diffuse reflectance spectra (DRS) were measured in a Shimadzu UV-3600 spectrophotometer equipped with a 5 cm diameter integrating sphere. The samples were ground in the agate mortar with barium sulfate in the weight ratio of 1 : 50. $BaSO_4$ was also used as a reference.

The upconversion luminescence spectra of the thin film samples were obtained using a 980 CW diode laser (LambdaWave) with a light power of 0.84 W and an irradiated area of 8 mm^2 (light power density: 105 mW mm^{-2}) combined with SPEX Fluorolog 3.22 (Horiba) spectrofluorometer. The film samples were prepared using the same procedure as for the preparation of thin films for photocatalytic tests (see: Photocatalytic measurements: a part).

Photoelectrochemical measurements were performed using 0.1 mol per dm^3 KNO_3 water solution as an electrolyte in a three-electrode set-up. The working electrode was prepared by spreading an aqueous suspension of studied material on a transparent foil covered with indium–tin-oxide (ITO) and dried afterwards in a stream of warm air (*ca.* 40–50 °C). The silver chloride electrode and a platinum wire were used as reference and auxiliary electrodes, respectively. The measurements were carried out using a 980 nm laser diode with an output power of 0.84 W and the photoelectric spectrometer and potentiostat (Instytut Fotonowy).

Photocatalytic measurements

Terephthalic acid (TA) was used as a reagent to investigate the photocatalytic activity of the materials. The fluorescence intensity (at λ_{max} = 426 nm) of hydroxyterephthalic acid (TAOH) formed in the reaction of TA hydroxylation was measured. We studied the photocatalytic activity of several samples in the form of suspended powders and thin films in various arrangements, and the following abbreviations for the prepared samples were used:

– UCPs@TiO_2(s) – suspension of $NaYF_4$:Yb^{3+},Tm^{3+} crystals coated with solvothermally synthesized titania;

– UCPs@TiO_2(f) – a thin film of $NaYF_4$:Yb^{3+},Tm^{3+} crystals coated with solvothermally synthesized titania;

– UCPs + P25(f) – a thin film of $NaYF_4$:Yb^{3+},Tm^{3+} crystals mixed with commercially available titania – P25 (Evonik);

– UCPs/P25(f/s) – thin film of $NaYF_4$:Yb^{3+},Tm^{3+} crystals and suspension of P25;

– UCPs/P25(f/f) – thin film of $NaYF_4$:Yb^{3+},Tm^{3+} crystals with an adjacent thin film of P25;

– UCPs + P25(s) – suspension of a mixture of $NaYF_4$:Yb^{3+},Tm^{3+} crystals, and P25.

Photocatalytic tests performed for thin films

Typically, 1.5 ml of the 0.3 mM TA solution in 10 mM NaOH aqueous solution was added to the glass cuvette. The UCPs + P25(f) sample was prepared by mixing 2 mg of the UCPs and 1 mg of P25 in a mortar and loaded on a thin transparent ITO foil. For the UCPs@TiO_2(f) sample, 3 mg of the material was used for one sample. The prepared film was then immersed in the TA solution and irradiated with a 0.84 W 980 nm laser diode. The cuvette was air-cooled, so the temperature rise of the suspension did not exceed 50 °C. In the experiment with the two separated thin films (UCPs/P25(f/f)), 2 mg of UCPs and 1 mg of P25 were used for the preparation of the films, respectively. The film with P25 was then immersed in the TA solution and the film with UCPs was placed in front of a cuvette. The whole setup was irradiated with a 0.84 W 980 nm laser diode. To determine the amount of generated TAOH, proportional to the amount of generated $HO^{\bullet}$ radicals, the fluorescence of the generated TAOH was measured every 30 minutes.

Photocatalytic tests performed on suspensions

The experiments with suspensions were conducted in the same conditions as for the thin films. Materials were suspended in 1.5 ml of the 0.3 mM TA solution in 10 mM NaOH aqueous solution and irradiated with the 980 nm laser diode. For the UCPs@TiO_2(s), 3 mg of the material was used. In the case of a UCPs/P25(f/s) sample, 1 mg of P25 was suspended in a solution, while 2 mg of UCPs was loaded on a transparent ITO foil in the form of a thin film, which was then placed in front of a cuvette. For a UCPs + P25(s) sample, 1 mg of P25 and 2 mg of UCPs were suspended in the same solution. Five identical samples were prepared and irradiated for 30, 60, 90, 120 and 150 minutes for each material. After that, the suspensions were collected and centrifuged to remove the photocatalyst and UCPs, and then the emission spectrum of the supernatant was measured.

Conclusions

We synthesized well-defined hexagonal $NaYF_4$:Yb^{3+},Tm^{3+} microcrystals (UCPs) exhibiting upconverting properties. Upon 980 nm irradiation, they emit intense UV and visible light, making them perfect candidates for use in NIR-driven photocatalysis. We combined UCPs with a photocatalyst by coating titania directly on their surface in the hydrothermal process and by preparing a physical mixture with commercially available TiO_2 (P25, Evonik). The obtained materials were characterized by SEM, EDX, XRD and photoluminescence spectroscopy. We studied the photocatalytic and photoelectrochemical activity of such UCPs-based photocatalytic systems in various experimental setups. We have discovered that the most efficient way to increase the photocatalytic activity of the studied materials is to prepare them in the form of thin films. An additional advantage of the proposed approach is the possibility of using microcrystalline UCPs, which are relatively easy to prepare and more efficient in NIR upconversion compared to their nanocrystalline analogues. We also proved that TiO_2 can be excited by the upconverted light without any direct physical contact between the photocatalyst and the upconverter, as demonstrated by the samples where a cuvette wall spatially separates the photocatalyst and UCPs. Such design allows for the creation of interchangeable and reusable NIR-driven photocatalytic systems.

Data availability

The data supporting this article have been included as part of the ESI.†

Author contributions

Paulina O'Callaghan: investigation, validation, visualization, writing – original draft; Agnieszka Jarosz-Duda: investigation, validation, visualization, writing – original draft; Joanna Kuncewicz: methodology, investigation, writing – original draft, writing – review and editing; Krzysztof Dzierżęga: investigation, validation; Wojciech Macyk: funding acquisition, project administration, methodology, writing – review and editing.

Conflicts of interest

There are no conflicts to declare.

Acknowledgements

This research was financially supported by the Foundation for Polish Science within the TEAM project (POIR.04.04.00-00-3D74/16).

References

1 L. Wang, X. Xu, Q. Cheng, S. X. Dou and Y. Du, *Small*, 2019, 1904107.
2 W. Wei, M. Ding, C. Lu, Y. Ni and Z. Xu, *Appl. Catal., B*, 2014, **144**, 379–385.
3 W. Shijia, J. Lv, F. Wang, N. Duan, Q. Li and Z. Wang, *Sci. Rep.*, 2017, **7**, 1–11.
4 S. M. Zheng, L. Li, K. Wang, R. Qiao, Y. Zhong, Y. Hu and Z. Li, *J. Mater. Chem. A*, 2014, **2**, 13486–13491.
5 W. Wanni, M. Zhao, C. Zhang and H. Qian, *Chem. Rec.*, 2020, **20**, 2–9.
6 X. Liu, C.-H. Yan and J. A. Capobianco, *Chem. Soc. Rev.*, 2015, **44**, 1299–1301.
7 Y. Sang, H. Liu and A. Umar, *ChemCatChem*, 2015, **7**, 559–573.
8 Y. Wu, S. Y. Chan, J. Xu and X. Liu, *Chem.–Asian J.*, 2021, **16**, 2596–2609.
9 C. Li, F. Wang, J. Zhu and C. Y. Jimmy, *Appl. Catal., B*, 2010, **100**, 433–439.
10 Q. Zhang, F. Yang, Z. Xu, M. Chaker and D. Ma, *Nanoscale Horiz.*, 2019, **4**, 579–591.
11 W. Yang, X. Li, D. Chi, H. Zhang and X. Liu, *Nanotechnology*, 2014, **25**, 482001.

12 A. Kar, S. Kundu and A. Patra, *ChemPhysChem*, 2015, **16**, 505–521.
13 D. Yin, L. Zhang, X. Cao, Z. Chen and J. Tang, *Dalton Trans.*, 2016, **45**, 1467–1475.
14 A. Jarosz-Duda, P. O'Callaghan, J. Kuncewicz, P. Łabuz and W. Macyk, *Catalysts*, 2020, **10**, 232.
15 A. A. Chilkalwar and S. S. Rayalu, *J. Phys. Chem. C*, 2018, **122**, 26307–26314.
16 H. Huang, H. Li, Z. Wang, P. Wang and Z. Zheng, *Chem. Eng. J.*, 2019, **361**, 1089–1097.
17 Z. Xu, M. Quintanilla, F. Vetrone, A. O. Govorov, M. Chaker and D. Ma, *Adv. Funct. Mater.*, 2015, **25**, 2950–2960.
18 Y. Yang, P. Zhou, W. Xu, S. Xu, Y. Jiang, X. Chen and H. Song, *J. Mater. Chem. C*, 2016, **4**, 659–662.
19 X. Xu, Y. Sun, Q. Zhang, H. Cai, Q. Li and S. Zhou, *Opt. Mater.*, 2019, **94**, 444–453.
20 H. Anwer and J.-W. Park, *Appl. Catal., B*, 2019, **243**, 438–447.
21 Q. Zhang, F. Yang, Z. Xu, M. Chaker and D. Ma, *Nanoscale Horiz.*, 2019, **4**, 579–591.
22 B. S. Richards, D. Hudry, D. Busko, A. Turshatov and I. A. Howard, *Chem. Rev.*, 2021, **121**, 9165–9195.
23 X. Li, F. Zhang and D. Zhao, *Nano Today*, 2013, **8**, 643–676.
24 Y. Tang, W. Di, X. Zhai, R. Yang and W. Qin, *ACS Catal.*, 2013, **3**, 405–412.
25 W. Wang, Y. Li, Z. Kang, F. Wang and J. C. Yu, *Appl. Catal., B*, 2016, **182**, 184–192.
26 Y. Chen, S. Mishra, G. Ledoux, E. Jeanneau, M. Daniel, J. Zhang and S. Daniele, *Chem.–Asian J.*, 2014, **9**, 2415–2421.
27 D.-X. Xu, Z.-W. Lian, M.-I. Fu, B. Yuan, J.-W. Shi and H.-J. Cui, *Appl. Catal., B*, 2013, **142–143**, 377–386.
28 W. Wang, W. Huang, Y. Ni, C. Lu and Z. Xu, *ACS Appl. Mater. Interfaces*, 2014, **6**, 340–348.
29 T.-M. Liu, J. Conde, T. Lipiński, A. Bednarkiewicz and C.-C. Huang, *NPG Asia Mater.*, 2016, **8**, e295.
30 F. Wang, J. Wang and X. Liu, *Angew. Chem., Int. Ed.*, 2010, **49**, 7456–7460.
31 F. T. Rabouw, P. T. Prins, P. Villanueva-Delgado, M. Castelijns, R. G. Geitenbeek and A. Meijerink, *ACS Nano*, 2018, **12**, 4812–4823.
32 D. C. Hurum, A. G. Agrios, K. A. Gray, T. Rajh and M. C. Thurnaueret, *J. Phys. Chem. B*, 2003, **107**, 4545–4549.
33 N. Bogdan, F. Vetrone, G. A. Ozin and J. A. Capobianco, *Nano Lett.*, 2011, **11**, 835–840.
34 Z. Hou, Y. Zhang, K. Deng, Y. Chen, X. Li, X. Deng, Z. Cheng, H. Lian, C. Li and J. Lin, *ACS Nano*, 2015, **9**, 2584–2599.